Characterization of DNA-wrapped carbon nanotubes by resonance Raman and optical absorption spectroscopies

C. Fantini [a,*], A. Jorio [a,b], A.P. Santos [c], V.S.T. Peressinotto [c], M.A. Pimenta [a]

[a] *Departamento de Física, Universidade Federal de Minas Gerais, Belo Horizonte, MG 30123-970, Brazil*
[b] *Materials Metrology Division, Brazilian National Institute of Metrology (INMETRO), Xerem, Duque de Caxias, RJ 25250-020, Brazil*
[c] *Centro de Desenvolvimento da Tecnologia Nuclear, Belo Horizonte, MG 30123-970, Brazil*

Abstract

Single-wall carbon nanotube (SWNT) samples grown by the CoMoCAT method are investigated by resonance Raman scattering and optical absorption. The environment effects in the population of the different (n,m) nanotubes present in the samples are characterized for DNA-wrapped nanotubes and the results are compared with SDS-wrapped CoMoCAT nanotubes. A significant decrease in the Raman intensity of metallic nanotubes is observed in the DNA-wrapped sample as compared to the SDS-wrapped sample, supporting the DNA-based separation method. This result is confirmed by optical absorption measurements in both samples.
© 2007 Elsevier B.V. All rights reserved.

1. Introduction

The production of carbon nanotube samples with well defined (n,m) tube type distribution is one of the most important goals in the field. Specially, the metallic vs. semiconducting separation is crucial for applications. Beside the development of separation methods, the development of a precise method to characterize the abundance of the different (n,m) species present in a sample is definitely necessary. SWNT samples, grown by Co–Mo catalysts (CoMoCAT), within bundles and dispersed in sodium dodecyl sulfate (SDS) suspension have been previously investigated by resonance Raman spectroscopy, where the (n,m) population for nanotubes dispersed in SDS solution was determined [1].

In this work we present a complete resonance Raman characterization of DNA-wrapped carbon nanotubes samples dispersed in aqueous solution in the region from 1.82 to 2.71 eV. The Raman results obtained for DNA-wrapped nanotubes, compared with those obtained for SDS-wrapped nanotubes [1], reveal that the Raman intensities for metallic nanotubes change substantially by changing the wrapping agent, while the results for semiconducting tubes remain the same. A reduction in the total Raman intensity for metallic nanotubes by about three times is observed in the DNA-wrapped sample when compared to the SDS-wrapped sample, showing that a semiconducting enriched nanotube solution is obtained when the nanotubes are dispersed in DNA. This result reinforces the assumption that DNA can be used to metal/semiconducting SWNT chromatographic separation, previously observed by Raman measurements [2] and predicted by theoretical calculations [3].

For a complementary characterization of the sample, analysis of the optical absorption spectra is also presented here. Usually, the separation is difficult to be observed with optical absorption because the metallic and semiconducting signals overlap. Methods to determine the nanotube population of (n,m) species based on the analysis of optical absorption spectra have been recently proposed [4,5], but the fitting of the optical absorption spectra is not trivial because in general each feature is a sum of the absorption

---

* Corresponding author.
E-mail address: cfleite@fisica.ufmg.br (C. Fantini).

peaks of several different nanotubes. However, a better analysis of the optical absorption spectra can be obtained when combined with Raman results. The optical absorption spectra for the two samples investigated here are analyzed by using a procedure based on the assignments made by the Raman study.

2. Experimental details

Resonance Raman experiments have been performed at room temperature and pressure using a DILOR XY triple-monochromator in a backscattering configuration, equipped with a liquid N_2 cooled charge coupled device (CCD). The samples were excited by a tunable laser system composed by a dye laser, with three different dye solutions (Rhodamine 110, Rhodamine 6G, and DCM special) that allow us to change continuously the laser excitation energy in the range 1.82–2.30 eV and an Ar–Kr ion laser, that provide 10 laser lines in the 2.34–2.71 eV range. A total of 65 different laser lines were used in the experiments. For each laser line the Raman spectrum of CCl_4 was also obtained and its intensity was used to normalize the intensity of the SWNT spectra obtained for each laser line. Optical UV–Vis absorption spectra were recorded using a Shimadzu UV-PC spectrophotometer in the 400–750 nm wavelength range. A carbon nanotube sample synthesized by CoMoCAT method [6] was used in the experiments. The DNA-wrapped SWNTs were obtained by sonication of CoMoCAT nanotubes in the presence of GT-DNA oligomers, followed by centrifugation at 15,000 rpm for 30 min. The preparation of SDS-wrapped CoMoCAT SWNTs used in the experiments has been described in reference [1].

3. Results

3.1. Raman measurements

From the measurements of the radial breathing mode frequency (ω_{RBM}) for different semiconducting and metallic nanotubes with different chiral indices (n,m) in the DNA-wrapped CoMoCAT nanotube sample, we obtained the two-dimensional map of E_{laser} vs. ω_{RBM} shown in Fig. 1a, where the color scale represents a linear scale of the intensities. We can see on the map high intensities associated with nanotubes $(6,4)$, $(6,5)$, $(7,5)$ and $(8,3)$, in agreement with SWNT + SDS results [1]. On the other hand, the intensity is much lower for metallic nanotubes, when compared with the SDS-wrapped sample results. When we represent the intensity of the Raman map on a logarithmic scale Fig. 1b many other optical transitions related to E_{22}^S and E_{11}^M can be observed. From the analysis of the experimental data, we obtained the optical transition energies (E_{ii}) associated with each (n,m) nanotube. The circles in Fig. 1b represent the E_{ii} vs. ω_{RBM} for each (n,m) nanotube after the analysis of the resonance behavior of each RBM peak, as explained in Ref. [7], and the numerical values
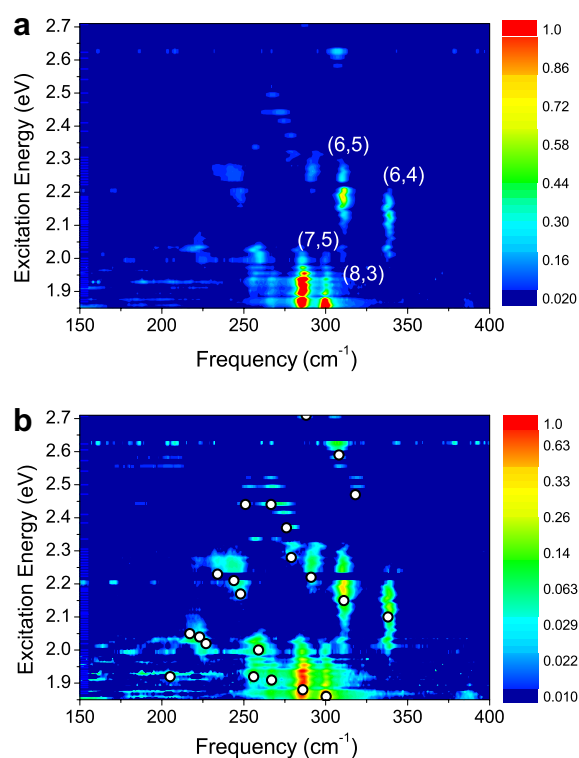

Fig. 1. Two-dimensional map obtained from the RBM Raman spectra of the DNA wrapped CoMoCAT carbon nanotube sample, by changing the laser excitation energy from 1.85 eV to 2.71 eV. The intensity is given by a linear color scale (a) and a logarithmic color scale (b). The white circles in (b) are the results of E_{ii} obtained from the analysis of the spectra. (For interpretation of the references to colour this figure legend, the reader is referred to the web version of this article.)

are shown in Table 1. The results obtained on SDS-wrapped CoMoCAT sample [1] are also shown in Table 1. A general behavior observed in Table 1 is that the RBM frequency for DNA-wrapped CoMoCAT nanotubes exhibits a small up-shift ($\Delta\overline{\omega}_{RBM} = 1.3\ cm^{-1}$) when compared with the SDS-wrapped CoMoCAT nanotubes, and also when compared with SDS-wrapped and bundled HiPco nanotubes (see Ref. [7]). Although this is a small number, it is a real effect since it was observed for most of the RBMs obtained with different laser lines, and calibrated by the CCl_4 spectra. This result indicates a different interaction between the DNA and the nanotube when compared to SDS.

The resonance Raman profiles were obtained from the plot of the intensity of each RBM peak as a function of the laser energy E_{laser}. Fig. 2 represents the resonance Raman profiles for the four strongest RBM features observed in Fig. 1a. The experimental intensities of the resonance Raman profiles observed in Fig. 1 are also shown in Table 1. These values have been normalized in order to make the sum of the intensities of all resonance Raman profiles equal to 100 and, thus, corresponds to the percent relative intensity of the resonance Raman profile associated with each (n,m) nanotube. After correcting for the (n,m) dependence of the Raman cross section [8], these numbers should represent the (n,m) population in one sample [1,9].

Table 1
Experimental values for the optical transition energies (eV), RBM frequencies (cm^{-1}) and RBM resonance Raman profile intensities (normalized to give 100 for the sum of all intensities) for the SDS (Ref. [1]) and DNA-wrapped (this work) CoMoCAT nanotube samples

(n,m)	SDS			DNA		
	E_{22}^{S}	ω_{RBM}	I_{RBM}^{Exp}	E_{22}^{S}	ω_{RBM}	I_{RBM}^{Exp}
(6,4)	2.09	337	5.57	2.10	338	6.98
(6,5)	2.18	309	10.82	2.15	311	11.85
(7,5)	1.88	284	21.81	1.88	286	27.38
(7,6)	1.90	266	1.78	1.89	267	2.74
(8,3)	1.87	299	25.45	1.85	300	32.86
(9,2)	2.23	291	1.09	2.22	291	2.33
(10,3)	1.90	254	1.53	1.92	256	1.70
(11,1)	2.00	259	1.60	2.03	259	1.75
(n,m)	E_{11}^{M}	ω_{RBM}	I_{RBM}^{Exp}	E_{11}^{M}	ω_{RBM}	I_{RBM}^{Exp}
(6,6)	2.69	288	1.44	2.71	288	0.79
(7,4)	2.58	308	8.08	2.59	308	1.62
(7,7)	2.43	250	1.10	2.44	251	0.63
(8,2)	2.45	318	2.76	2.45	318	0.55
(8,5)	2.47	265	2.46	2.44	267	1.15
(9,3)	2.35	274	3.30			
(9,6)	2.23	233	0.29	2.23	234	0.85
(9,9)	2.03	198	0.10			
(10,1)	2.28	280	5.50	2.28	279	1.23
(10,4)	2.20	242	0.71	2.21	244	1.20
(11,2)	2.19	245	2.17	2.17	248	1.23
(11,5)	2.06	215	0.15	2.05	217	0.41
(12,0)	2.16	247	0.87			
(12,3)	2.04	220	0.23	2.04	223	0.90
(13,1)	2.02	224	0.27	2.02	227	1.10
(14,2)	1.92	202	0.87	1.92	205	0.74

The values for semiconducting and metallic nanotubes are shown on the top part and the bottom parts of the table, respectively.
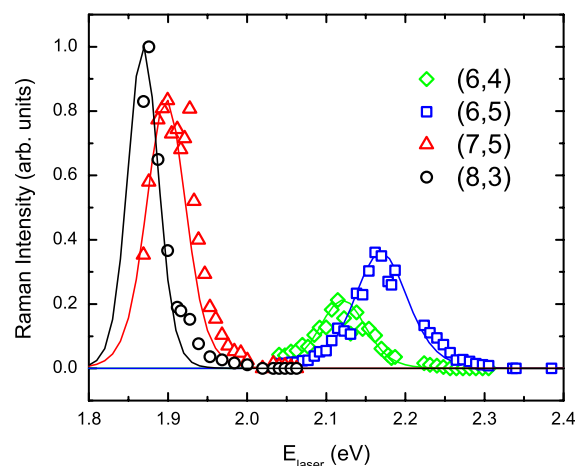

Fig. 2. Resonance Raman profiles obtained for the four most intense radial breathing modes observed in Fig. 1a, associated with the (6,4), (6,5), (7,5) and (8,3) nanotubes. The line-width of the resonance windows are 70, 85, 60, and ~40 meV, respectively.

However, since we are interested in comparing the metallic vs. semiconducting behavior, we will consider hereafter only the experimental values, which do not involve the adoption of any theoretical model for the Raman cross-section.

Fig. 3 shows the resonance profile intensities obtained from Table 1 for the semiconducting nanotubes as a function of nanotube diameter Fig. 3a and chiral, angle Fig. 3b and for the metallic nanotubes as a function of nanotube diameter Fig. 3c and chiral angle Fig. 3d. The black and gray bars represent the results for DNA-wrapped
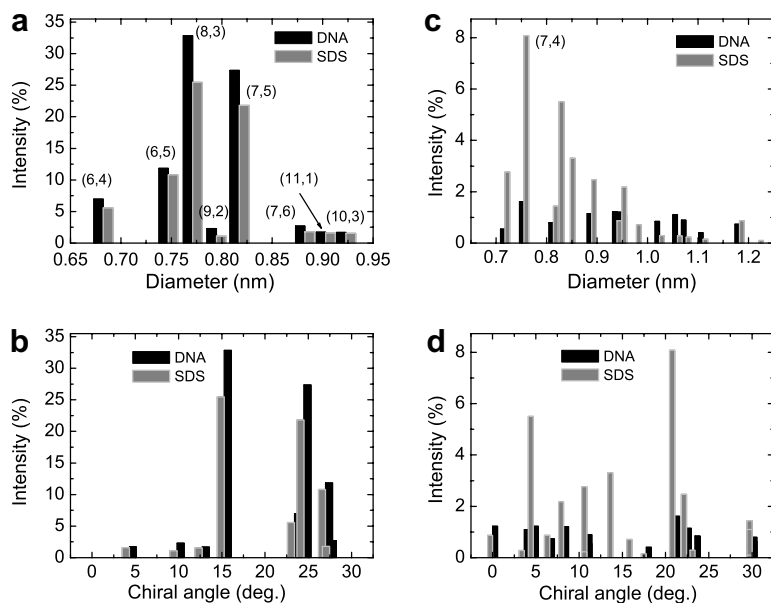

Fig. 3. Dependence of the resonance profile intensity for different semiconducting nanotubes (a) on the diameter and (b) on the chiral angle. Dependence of the resonance profile intensity for different metallic nanotubes (c) on the diameter and (d) on the chiral angle. SDS-wrapped and DNA-wrapped nanotubes are represented by gray bars and black bars, respectively. Results are given as a percentage of the overall (semiconducting plus metallic) intensity.

(this work) and SDS-wrapped [1] samples, respectively. We can see in Figs. 3a and 3b that the intensities of the Raman profiles for the semiconducting nanotubes are practically the same for the DNA and SDS-wrapped samples. The slightly smaller percent intensities for SDS-wrapped tubes, when compared to DNA-wrapped ones, is a consequence of the clearly larger contribution from metallic tubes in the SDS-wrapped sample when compared to the DNA-wrapped one as discussed below.

For the metallic nanotubes, the intensities are much lower for the DNA-wrapped sample when compared with the SDS-wrapped one, mainly in the low-diameter range. In the large diameter range some metallic DNA-wrapped SWNT, such as $(9,6)$ exhibit higher intensity than in SDS-wrapped sample (see Table 1), due to the diameter dependence of the intensities of metallic SDS-wrapped SWNT observed in Fig. 3c. The sum of the intensities of the resonance profiles for all metallic nanotubes in the SDS-wrapped sample corresponds to ~1/3 of the total intensity, while in DNA-wrapped sample it corresponds to ~1/9 of the total intensity.

3.2. Optical absorption

In this section the optical absorption results obtained for both DNA- and SDS-wrapped samples are presented and compared with that obtained by resonance Raman spectroscopy. The analysis of the optical absorption spectrum for the DNA-wrapped nanotube sample is shown in Fig. 4a. In this Fig. 4a we can see the contribution of several (n,m) nanotubes for the optical absorption features, considering the energy range between 1.8 and 2.7 eV. For comparison, we show in Fig. 4b the optical absorption spectrum for the SDS-wrapped CoMoCAT nanotube sample used in our previous population analysis [1].

The optical absorption spectra has been analyzed considering the results obtained from Raman spectroscopy. Fig. 4c shows an E_{ii} vs. ω_{RBM} plot for the experimental data obtained in Fig. 1 where black circles and gray squares represent the semiconducting and metallic tubes, respectively. The theoretical data from the extended tight-binding model including many-body corrections are also shown in the figure represented by '×' symbols [10]. Fig. 4d presents the optical absorption spectrum for the DNA-wrapped CoMoCAT sample, in the same energy range of Fig. 4c. The solid (dashed) arrows connect each different semiconducting (metallic) nanotube in Fig. 4c with its contribution to the optical absorption features. Four main bands are observed in the optical absorption spectra. The first band (around 1.9 eV) is composed mainly by contributions from the $(7,5)$, $(7,6)$ and $(8,3)$ semiconducting nanotubes, with a small contribution from the $(14,2)$ metallic nanotube. The second band in the optical absorption spectra, between 2.0 and 2.3 eV, is composed of contributions associated with both semiconducting and metallic nanotubes, while the third band, around 2.4 eV, is associated basically with optical
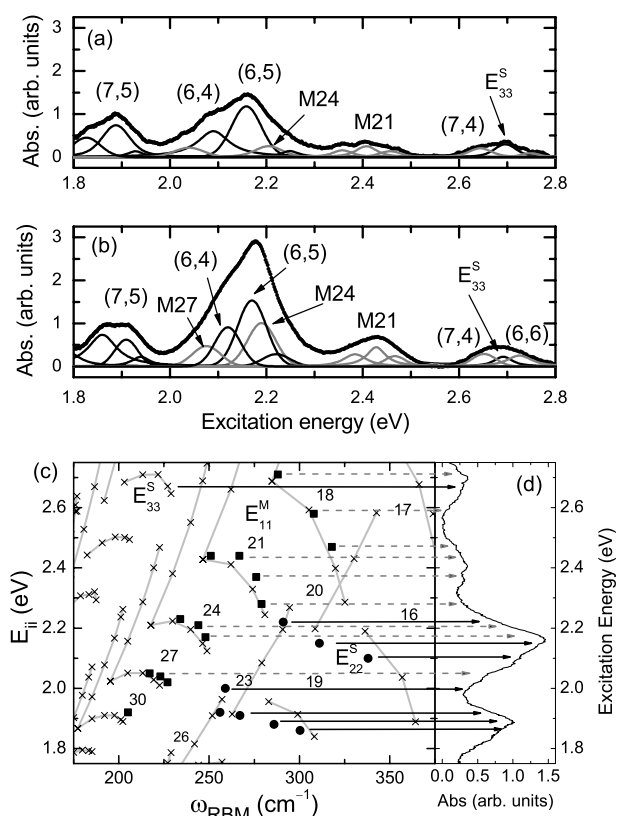

Fig. 4. Analysis of the optical absorption spectra for the DNA-wrapped (a) and SDS-wrapped (b) samples. Black and gray features are associated with semiconducting and metallic nanotubes, respectively. (c) E_{ii} vs. ω_{RBM} plot. The black circles and gray squares represent the experimental data for semiconducting and metallic nanotubes, respectively, in the DNA-wrapped sample. × symbols represent values from Ref. [10]. (d) Optical absorption spectra for the DNA-wrapped nanotubes in the same energy range of the Raman measurements. The solid (dashed) arrows connect the semiconducting (metallic) nanotubes in the E_{ii} vs. ω_{RBM} plot to their contribution in the optical absorption spectrum.

absorptions by metallic nanotubes in the E_{11}^{M} region. Finally, the fourth band (around 2.7 eV) is related to absorptions by both metallic and semiconducting nanotubes in the E_{11}^{M} and E_{33}^{S} regions, respectively. Note that some low intensity peaks in this E_{33}^{S} region are indeed observed in the Raman measurements (see Fig. 1b).

According to Raman results, the SDS and DNA-wrapped samples exhibit a similar amount of semiconducting nanotubes. Thus, in the analysis of the optical absorption spectra, the intensities for DNA-wrapped and SDS-wrapped samples can be normalized by the intensity of the first band (~1.9 eV), originating mostly from contributions from semiconducting nanotubes. In the analysis of the absorption spectra, the bands associated with semiconducting nanotubes present the same intensities in both samples, as we can see for the features indicated in Fig. 4a and b associated with nanotubes $(6,5)$, $(6,4)$ and $(7,5)$. The line-width (FWHM) for the optical absorption features, that are predicted to be (n,m) dependent [11], have been considered in the analysis to be the same as obtained for the RBM resonance Raman profiles (Fig. 2).

The absorption features associated with metallic nanotubes exhibit lower intensities for the DNA-wrapped sample (Fig. 4a) when compared with the SDS-wrapped sample (Fig.4b). In the second band the semiconducting peaks show the same intensity in the two samples, while the metallic features associated with the families $2n + m = 24$ and 27, indicated in Fig. 4a and b by M24 and M27, respectively, are strongly decreased in the DNA-wrapped sample. The third band in the optical absorption spectra, indicated by M21, associated basically with metallic nanotubes from family $2n + m = 21$ (and a small contribution from $2n + m = 18$) is also reduced in the DNA-wrapped sample. The same effect is observed for the highest energy band where the intensities for the features associated with metallic nanotubes from family $2n + m = 18$ are decreased, while the feature associated with the E_{33}^S optical absorption exhibits the same intensity in the spectra for both samples.

Thus, the optical absorption results show a reduction in the intensity for metallic nanotubes in agreement with resonance Raman measurements, revealing a reduction in the amount of metallic nanotubes when the nanotubes are dispersed with DNA instead of the SDS surfactant. The intensities of metallic nanotubes correspond to 1/3 of the total intensity of the absorption spectrum for the SDS-wrapped sample and 1/6 of the total intensity for the DNA-wrapped sample, that although is not the same value obtained by the Raman measurements it reveals a reduction in the amount of metallic nanotubes. It must be emphasized that the resonance Raman and the optical absorption intensities are not proportional to the relative population of the (n, m) nanotubes present in the sample, since both intensities depend in a different way of the (n, m) nanotube species [9]. Moreover, in the optical absorption spectra the $(6, 5)$ nanotube exhibit the most intensive feature, due to the higher population of this nanotube in the samples, as can also be obtained by the ratio between the experimental and calculated intensities as discussed in Refs. [1,8]. The results show a good agreement between Raman and optical absorption measurements when combined for characterization of the nanotube sample population.

4. Conclusions

In summary, CoMoCAT nanotube samples wrapped with different surfactant (DNA and SDS) were characterized by resonance Raman and optical absorption spectroscopies. The experimental results reveal different interactions for semiconducting and metallic nanotubes depending on the type of surfactant used. Despite the fact that the determination of the absolute semiconducting to metal population rate depends on the Raman cross-section calculation, the large enrichment of semiconducting vs. metallic tubes ($\sim$3 times) when using DNA as a surfactant can be directly seen from the resonance Raman profiles. The result is confirmed by the analysis of the optical absorption spectra that, when combined with Raman results, provides a precise characterization of nanotube samples and probes the separation process induced by the DNA-wrapping.

References

[1] A. Jorio et al., Phys. Rev. B 72 (2005) 075207.
[2] S.G. Chou et al., Chem. Phys. Lett. 397 (2004) 296.
[3] S.R. Lustig, A. Jagota, C. Khripin, M. Zheng, J. Phys. Chem. B 109 (2005) 2559.
[4] N. Nair, M.L. Usrey, W.-J. Kim, R.D. Braatz, M.S. Strano, Anal. Chem. 78 (2006) 7689.
[5] Z. Luo, L.D. Pfefferle, G.L. Haller, P. Papadimitrakopoulos, J. Am. Chem. Soc. 128 (2006) 15511.
[6] B. Kitiyanan, W.E. Alvarez, J.H. Harwell, D.E. Resasco, Chem. Phys. Lett. 317 (2000) 497.
[7] C. Fantini, A. Jorio, M. Souza, M.S. Strano, M.S. Dresselhaus, M.A. Pimenta, Phys. Rev. Lett. 93 (2004) 147406.
[8] J. Jiang et al., Phys. Rev. B 71 (2005) 205420.
[9] A. Jorio et al., Appl. Phys. Lett. 88 (2006) 023109.
[10] A. Jorio et al., Phys. Rev. B 71 (2005) 075401.
[11] J.S. Park et al., Phys. Rev. B 74 (2006) 165414.